



Molecular properties and potential energy surfaces of the cyanides of the groups 1 and 11 metal atoms

Dong-Ki Lee, Ivan S Lim, Yoon Sup Lee, Denis Hagebaum-Reignier,
Gwang-Hi Jeung

► To cite this version:

Dong-Ki Lee, Ivan S Lim, Yoon Sup Lee, Denis Hagebaum-Reignier, Gwang-Hi Jeung. Molecular properties and potential energy surfaces of the cyanides of the groups 1 and 11 metal atoms. *Journal of Chemical Physics*, 2007, 10.1063/1.2749504 . hal-03561424

HAL Id: hal-03561424

<https://hal.science/hal-03561424>

Submitted on 8 Feb 2022

HAL is a multi-disciplinary open access archive for the deposit and dissemination of scientific research documents, whether they are published or not. The documents may come from teaching and research institutions in France or abroad, or from public or private research centers.

L'archive ouverte pluridisciplinaire **HAL**, est destinée au dépôt et à la diffusion de documents scientifiques de niveau recherche, publiés ou non, émanant des établissements d'enseignement et de recherche français ou étrangers, des laboratoires publics ou privés.

Molecular properties and potential energy surfaces of the cyanides of the groups 1 and 11 metal atoms

Dong-ki Lee, Ivan S. Lim, and Yoon Sup Lee^{a)}

Department of Chemistry, Korea Advanced Institute of Science and Technology, 305-701 Daejeon, Korea
and School of Molecular Sciences (BK21), Korea Advanced Institute of Science and Technology,
305-701 Daejeon, Korea

Denis Hagebaum-Reignier and Gwang-Hi Jeung^{b)}

Chimie Théorique, Case 521 (CNRS, UMR 6517), Université de Provence, Campus de Saint-Jérôme,
13397 Marseille Cedex 20, France

(Received 4 January 2007; accepted 22 May 2007; published online 29 June 2007)

Ab initio calculations on the metal (groups 1 and 11) cyanide complexes show two stable configurations for the ground state geometry, a linear cyanide (MCN) and a triangular (MNC) form with an obtuse M–N–C angle. Lithium complex may exist in a linear isocyanide (MNC) form, but it cannot be differentiated from the triangular configuration because of the flatness of the potential energy surface connecting the two isomers. The metal atom and cyano radical are bonded through a strongly ionic configuration (M^+CN^-) in both geometrical forms. The MNC triangular form is a very floppy structure having one low frequency for the bending mode, whereas the MCN linear form is more rigid. The CN complexes of the alkali atoms have a triangular geometry as the lowest energy conformer, while the noble metal atoms prefer the linear cyanide one. The relative stability of the two isomers, dipole moments, and effective charges are reported in this paper. The essential aspects of the potential energy surfaces for the ground and the first excited states exhibiting a closely avoided crossing are also explained. © 2007 American Institute of Physics.

[DOI: [10.1063/1.2749504](https://doi.org/10.1063/1.2749504)]

I. INTRODUCTION

The relative stability between different conformers of cyanide complexes of a metal atom has been a subject to many scientific investigations by quantum mechanical calculations.^{1–6} There are the linear cyanide (MCN), linear isocyanide (MNC), and the triangular (sometimes written as $M[CN]$) forms. They are characterized by a monocoordination (monohapto, η^1 according to the organometallic notation) for the linear two forms and a bicoordination (dihapto, η^2) for the triangular form. Historically, the first infrared absorption spectra of the triatomic cyanides of Na and K were observed by Leroi and Klemperer.⁷ They noted that the C–N stretching frequency (ν_3) in XCN (X=H, Na, K, Cl, Br, and I), in general, appeared rather insensitive to the nature of the X atom and reported the measured values of 2176 ± 5 and 2158 ± 5 cm^{-1} for NaCN and KCN, respectively, which assumed a linear cyanide configuration, in comparison with the free CN value⁸ of 2068.59 cm^{-1} . However, they also observed low-frequency vibrations at 239 ± 10 and 207 ± 20 cm^{-1} for NaCN and KCN, respectively. These bands were presumably assigned to the bending mode (ν_2). More than a decade later Ismail *et al.*⁹ found linear geometries for the cyanides of Li, Na, and K atoms from isotopic substitutions and reported frequencies for the three modes of vibration from their matrix-isolation study. Their bending frequencies, however (119 , 168 , and 139 cm^{-1} for LiCN, NaCN, and

KCN, respectively), were much smaller than those reported earlier by Leroi and Klemperer. Later, van Vaals *et al.*¹⁰ and Törring *et al.*¹¹ have reported the microwave absorption and molecular-beam electric-resonance rotational spectra of the gaseous Li, Na, and K cyanides. These studies suggested a nonlinear bent form (or a *T* form) as the ground state geometry for the Na and K complexes while a linear isocyanide form was concluded to be most stable for the Li complex. The M–C distance was slightly longer than the M–N distance, while the C–N distance showed a little variation from that of free cyanide [$r_e(\text{C–N}) = 1.170(4)$ and $1.162(10)$ Å for NaCN and KCN, respectively, in comparison with $1.1718(2)$ Å for free cyanide, see Ref. 8]. To the best of our knowledge, no experimental or theoretical data were reported on RbCN, CsCN, or FrCN.

For the light alkali metal cyanide complexes early *ab initio* calculations showed that LiCN was most stable in the isocyanide configuration at the Hartree-Fock (HF) level²⁴ with a small isomerization energy to the cyanide conformer (8.8 kcal/mol). The barrier height between the two conformers was calculated to be lower at the correlated level due mainly to the stabilization of the cyanide form.¹² The extreme floppiness of LiCN was discussed more recently by studying a wide domain of the potential energy surface (PES).⁵ For the T-shape cyanide complexes such as NaCN and KCN, the electron correlation effects were found to be particularly important for determining the M–N–C angle, which became smaller by up to 10% at the third-order Møller-Plesset perturbation (MP3) level of theory.³ It is in-

^{a)}Electronic mail: yoonsuplee@kaist.ac.kr

^{b)}Electronic mail: jeung@up.univ-mrs.fr

deed well known that the overall stability order among different isomers is sensitive to the basis set and the method used. The potential energy surfaces for the isomerizations of $\text{HCN} \leftrightarrow \text{HNC}$ and $\text{LiCN} \leftrightarrow \text{LiNC}$ are available, which were obtained at the second-order Møller-Plesset perturbation (MP2) and quadratically convergent configuration interaction singles-and-doubles levels of theory.¹³ Farantos and Tennyson¹⁴ have reported a trajectory calculation for the LiCN and KCN systems with two degrees of freedom neglecting the C–N vibrations, where the metal atom appeared to move around the CN group in a chaotic way.

As for the group 11 metal complexes from Cu to Au, there are several articles^{15–20} that can be found in the literature since the first *ab initio* calculation of CuCN by Bauschlicher.²¹ These studies concluded that all cyanide complexes of the group 11 metal prefer the linear cyanide structure. The photoelectron spectra of the anion¹⁹ and a gas-phase millimeter-wave spectroscopy²² showed the cyanide form of CuCN to be the only observed conformer. While AgCN was also elucidated by photoelectron spectra¹⁹ no reliable experiment was reported for AuCN. We note that the monocyanoanides of some other transition metal atoms and the alkaline earth atoms were also studied. Interested readers can find many useful references in a recent paper on NiCN by Paul *et al.*²³

The strong ionic bonding between an alkali atom and a cyanoradical has been pointed out in *ab initio* calculations by Bak *et al.*²⁴ We have recently pointed out some possible sources of errors in calculating the strength of ionic bonding and showed a way to remedy such error.²⁵

In this paper, we present high level *ab initio* calculations for the cyanides of the groups 1 (from Li to Fr) and 11 (from Cu to Au) metals obtained at the coupled-cluster and multi-reference configuration interaction (MRCI) levels using large flexible basis sets to describe both the ionic and covalent configurations. It is not easy to perform a highly accurate calculation for the MCN system by the reasons explained in this paper. However, by performing a larger scale calculation than previously attempted, we try to approach closer to the true order of chemical stability. Some of the properties of groups 1 and 11 complexes of cyanide are compared for different monovalent metal atoms. A wide range of the potential energy surfaces for the ground and a few excited states of the Li and Na complexes are calculated. The alkali cyanides have the ground state PESs which are quite flat for a fairly large domain of geometry, which leads to large amplitude vibrational motions. It is not the aim of this work to study such motions.

II. METHOD OF COMPUTATION

The *ab initio* HF, the MRCI, the coupled-cluster (CC) method, the second-order perturbation method using Møller-Plesset (MP) partition, and the density functional theory (DFT) calculations were performed using MOLCAS,²⁶ MOLPRO,²⁷ and GAUSSIAN03²⁸ program packages. Extended atomic basis sets were optimized to describe simultaneously the covalent and ionic configurations and the ground and excited states. The all-electron basis sets used consisted of

the following Gaussian type orbitals (GTOs): $13s8p3d$ for C, $12s7p3d$ for N, $15s10p6d3f$ for Li, $15s10p5d1f$ for Na, and $16s12p6d$ for K. These GTOs were used without contraction. Our basis for Li is larger than that of Na and that of K because we have calculated a larger number of the excited states for LiCN than NaCN and KCN. The *f* basis function does not significantly change the ground state energy for the alkali atoms. Molecular orbitals (MOs) resulting from the complete active space (CAS) self-consistent field (SCF) calculations were used for the correlation calculations at the MRCI level. State averaging was used to study the ground and excited states. In MRCI calculations, no virtual orbitals were excluded in generating the configuration state functions (CSFs). Only single excitations were allowed from the $1s^2$ core of the Li and the $2s^2$ electrons of C and N, while the rest of the valence electrons were allowed to make all possible single and double excitations. For the CC calculations, all valence electrons were correlated. The effective charge of each atom for triangular geometry was calculated from two components of the dipole moment together with the condition that the sum of the effective charges should vanish. The details about dipole moment vectors will be available for the interested readers.

The relativistic effects could be significant for the CN complexes of heavy metal atoms. We have done comparative nonrelativistic and relativistic HF calculations for (K to Fr)CN. We found that scalar relativistic effects shortens the M–C and M–N distances slightly, and increased slightly the vibrational frequencies with the largest change being 4.7 cm^{-1} for the bending frequency (ω_2) of FrCN. For K, Rb, Cs, and Fr, we used small-core (nine valence electron) energy-consistent *j*-averaged pseudopotentials of Lim *et al.*²⁹ For Cu, Ag, and Au, we have used small-core (19 valence electrons) energy-consistent pseudopotentials and the valence basis sets of Figgen *et al.*³⁰ The spin-orbit coupling was neglected in the present study.

The potential energy surfaces were calculated with the MRCI method. The critical points (minima, maxima, and saddle points) were initially located and then optimized by HF, CCSD and CCSD(T) methods and subsequently by MRCI. Harmonic vibrational frequencies of selected conformers were calculated at CCSD and CCSD(T). In describing the potential energy surfaces, the Jacobian coordinates (R, r, θ) were used where r is the C–N distance with the vector direction according to $\text{C} \leftarrow \text{N}$, R is the distance between the metal atom and the center of mass of CN (O) with the vector direction from O to M ($\text{O} \rightarrow \text{M}$), and θ is the angle between r and R ($\theta=0$ corresponds to the NCM linear geometry and $\theta=\pi$ corresponds to the MNC linear geometry).

Concerning the triatomic molecules made from three different atomic species (ABC), there is no generally accepted convention for the denomination of three fundamental vibrational frequencies ($\nu_1/\nu_2/\nu_3$). (Logical denomination could be according to the ascending or descending order of the frequency.) In the MCN cases, a majority of experimentalists have given the denomination according to the magnitudes following $\nu_2 < \nu_1 < \nu_3$. We are going to use this convention, although a different choice was also used in the literature. In the linear species, ν_3 is close to the vibrational frequency of

free C–N, 2068.59 cm^{-1} , thus representing essentially the C–N stretching and ν_1 can be interpreted as the stretching motion of the metal atom with respect to the CN moiety. As this study is not intended for calculating a large number of the vibrational levels, the $R(\text{C–N})$ is only slightly varied around the equilibrium distance.

III. RESULTS AND DISCUSSION

The cyano radical is a strongly electronegative molecule, its electron affinity being measured to be $3.862 \pm 0.004\text{ eV}$.³¹ The MRCI calculation for just the CN and CN[−] molecules alone gave the electron affinity of 3.787 eV. The same accuracy could be achieved at the CCSD(T) level. According to our calculation, the equilibrium internuclear distance (R_e) of the ground state of CN is 1.174 Å at the MRCI level, which is slightly longer than the experimental value, 1.1718(2) Å.⁸ The R_e of CN[−] is calculated to be 1.176 Å which agrees well with the experimental data, 1.177(4) Å.³¹ The chemical bond between a metal atom and a cyano radical is mainly made by an ionic bonding through an electron transfer from the metal atom towards the cyano radical.

To fully understand the interaction between the metal atom and the cyano radical, one requires not only the information on the ground state potential surface but also that on some excited states. In the case of LiCN and NaCN, three corresponding asymptotes in the increasing order in energy are $\text{M}+\text{CN}(X^2\Sigma^+)$, then $\text{M}+\text{CN}(A^2\Pi_r)$ which lies 9245.28 cm^{-1} higher than the former,⁸ followed by M^++CN^- . The energy level of M^++CN^- is $\Delta=\text{IP}(\text{M})-\text{EA}(\text{CN})$ with respect to the ground state dissociation asymptote of $\text{M}+\text{CN}(X^2\Sigma^+)$, where $\text{IP}(\text{M})$ is the ionization energy of the metal atom and $\text{EA}(\text{CN})$ is the electron affinity of CN. In the case of KCN, RbCN, CsCN, and FrCN, we need to know only the lowest two potential surfaces dissociating into $\text{M}+\text{CN}(X^2\Sigma^+)$ and M^++CN^- , respectively. To explain the essential features of the interaction between a metal atom and the CN we need to see different sections of the potential energy surfaces. Figure 1 shows several sections. A section of three potential energy surfaces of LiCN is shown in Fig. 1(a). In this section, r is fixed to 2.21 bohrs (about 117 pm) and θ is fixed to $\pi/2$. The lower broken curve represents $\Delta_{\text{th}}-R^{-1}$, where Δ_{th} is the MRCI calculated value for $\text{IP}(\text{Li})-\text{EA}(\text{CN})$, 0.048 150 hartree (1.3102 eV). The upper broken curve is $\Delta_{\text{expt}}-R^{-1}$, where Δ_{expt} is the experimental value, 0.056 209 hartree (1.5295 eV). The ground state ($1^1A'$) is attractive ionic for R up to 20.77 bohrs (110 pm) and it is nonbonding, $\text{M}+\text{CN}(X^2\Sigma^+)$ for larger R . The first excited state ($2^1A'$) is covalent and repulsive for $R < 20.77$ bohrs, attractive ionic for $20.77\text{ bohrs} < R < 49.3$ bohrs (261 pm) and is nonbonding [not shown in Fig. 1(a)], $\text{Li}+\text{CN}(A^2\Pi_r)$ for larger distances. The second excited state ($3^1A'$) is repulsive for $R < 49.3$ bohrs and attractive ionic [not shown in Fig. 1(a)] for larger distances to become M^++CN^- at infinity. The ionic-covalent avoided crossings occur punctually (i.e., well localized), and the energy splittings (or gaps) are very small as was reported in the case of NaCN.²⁵ The ionic parts of the potential energy surfaces closely follow the $\Delta_{\text{th}}-R^{-1}$ function (considering the

bond as a point-charge dipole) down to relatively short distances: in Fig. 1(a), the calculated curve is 0.000 188 hartree (0.005 eV) lower than the point-charge model at 10 bohrs, 0.000 094 hartree (0.003 eV) higher at 20 bohrs, and 0.000 031 hartree (less than 0.001 eV) higher at 30 bohrs. In reality, the ionic parts should rather follow the upper broken curve. As a consequence, the ionic-covalent avoided crossing distances should be located at smaller R 's than the above mentioned distances. The origin and the consequences (spectroscopic properties and reaction dynamic properties) of the inaccuracy of the *ab initio* and DFT calculations have been explained earlier.²⁵

Different sections of the ground state potential energy surface are reported in Fig. 1(b). Here, r is fixed and R and θ are varied. In Figs. 1(a) and 1(b), we have used six a' MOs and two a'' MOs to distribute six valence electrons (one from Li, two from C, and three from N) in the CASSCF (616 CSFs) then all possible single and double substitutions were taken into account in the MRCI (6 104 070 CSFs). We can see in Fig. 1(b) two stable conformers, linear LiCN and LiNC. The LiNC linear conformer appeared to be lower than the LiCN linear conformer by 0.0469 eV at this level of MRCI (which we will call MRCI-1). The potential energy changes little on bending the Li–N–C angle around $\theta=180^\circ$. Bending the Li–C–N angle around $\theta=0^\circ$ changes the potential energy more, resulting in a relatively higher bending frequency than in the former case. In a second MRCI, we have used five a' MOs and two a'' MOs to distribute six valence electrons in the CASSCF (260 CSFs), and then all possible single and double substitutions were considered. Furthermore, two more electrons from $5a'$ MO that correspond to a polarized $2s^2$ atomic orbital of the carbon atom were allowed to make all possible single substitutions, which made the dimension of CI to be 13 776 392 (we will call this MRCI-2). The result is slightly different, suggesting a significant correlation effect between the C ($2s^2$) electrons and other valence electrons. A triangular C_s geometry (T shape) with η^2 coordination appeared to be the most stable form, and the linear LiCN is 0.0125 eV higher than the former but is stable because of a potential barrier connecting these two conformers. The linear LiNC is unstable as there exists no potential barrier separating this from the triangular form. The lowest energy of the LiNC is 0.0333 eV higher than the triangular form. However, the triangular form has a much lower bending frequency in comparison with the linear LiCN as in the MRCI-1.

Our results as well as former theoretical studies demonstrate the difficulty of deciding the relative stability of three different conformers for LiCN complex. The relative stabilities of different conformers MCN are reported in Table I. The result differs according to the method of calculation, the atomic and molecular basis set and the level of correlation effect taken into account. The HF method does not give any stable triangular form but gives the linear LiNC lower than the linear LiCN, the transition state connecting these two forms being triangular. The inclusion of the electron correlation effect at the CCSD level gives a stable triangular form separated from the linear LiNC by a very low potential barrier. Inclusion of the higher order correlation effect by the

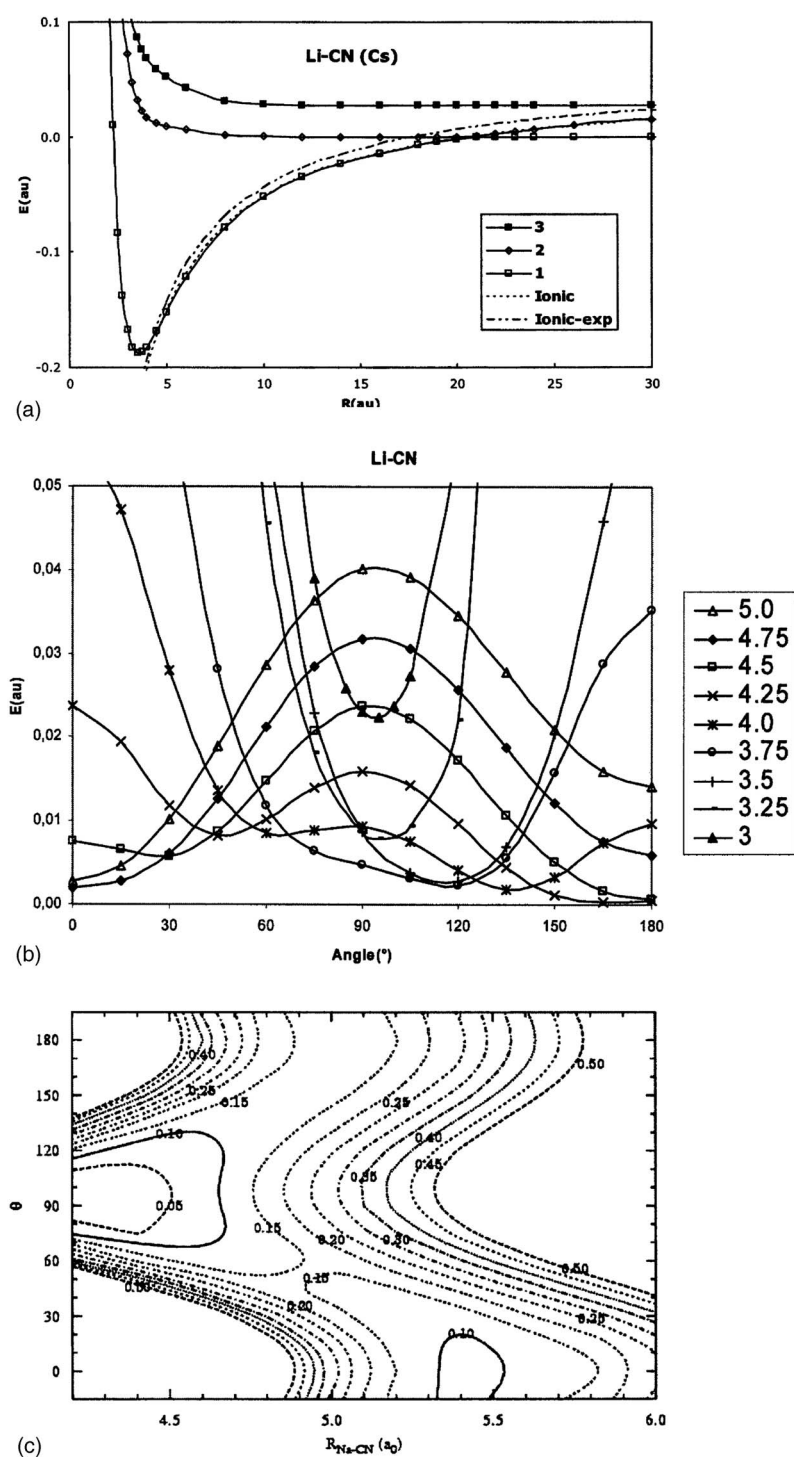


FIG. 1. (a) A C_3 section of potential energy surfaces of LiCN . The C-N distance (r) is fixed to 2.21 bohrs, the Jacobian angle (θ) is $\pi/2$, and R in bohr is the distance between Li and the center of mass of CN . Broken curves for $\Delta_{\text{expt}} - R^{-1}$ (upper curve) and $\Delta_{\text{th}} - R^{-1}$ (lower curve) are the point-charge curves (see text). (b) A section of the ground state potential energy surface where $r(\text{C-N}) = 2.21$ bohrs; R (legend, in bohr) and θ (abscissa, in degree) are varied. The energy scale is with respect to the lowest potential energy of the LiNC linear complex. (c) Isopotential (in eV) contour map for the ground state potential energy surface of NaCN in Jacobian coordinates with $r(\text{C-N}) = 2.21$ bohrs. Potential energies are with respect to the minimum value found in a triangular geometry.

CCSD(T) method gives the triangular form practically at the same energy level as the linear LiNC form. Considering the same tendency of relative energy change in the MRCI-1 and MRCI-2, we guess that more extensive inclusion of the correlation effect would give the triangular form as the lowest energy form and the linear LiNC should not be a stable form. The LiNC conformer or the triangular conformer is easy to bend around the Li-N-C angle of 150° (MRCI-2) so it is most likely that those two forms cannot be distinguished in reality when the dynamic aspect¹³ is taken into account. Table I shows that the ground state of the cyanides of alkali

atom appears to generally prefer the triangular (η^2) geometry. The M-CN bond energy decrease for the suite $\text{Li} \rightarrow \text{Na} \rightarrow \text{K}$ has been reported previously.²⁵

In contrast, the CN complexes of the group 11 metal atoms prefer the linear MCN geometry, the only other stable geometry being the linear MNC , as can be seen in Table I. These two conformers are connected by a transition state which is naturally a triangular form. The linear MCN form becomes more and more stable with respect to the linear MNC form for the $\text{Cu} \rightarrow \text{Ag} \rightarrow \text{Au}$ suite, and the height of potential barrier increases in the same order. The relative

TABLE I. Relative energy levels of the MCN complexes and the transition states (TSs) in kJ/mol (1 eV = 96.4853 kJ/mol and 1 hartree = 27.2107 eV). Saddle points are indicated by “#” and nonexistent data are indicated by “—.”

Atom	Method	MCN (linear)	TS1	M[CN] (η^2)	TS2	MNC (linear)
Li	HF	25.3	39.2	—	—	0
	CCSD	10.4	22.9	0.4	3.4	0
	CCSD(T)	8.8	20.6	0.1	2.9	0
	MRCI-1	4.5	—	—	—	0
	MRCI-2	1.3	—	0	—	3.2(#)
	MP2-4 ^a	6.9	—	1.2	—	0
Na	HF	16.8	22.5	0	2.5	2.2
	CCSD(T)	10.1	15.8	0	11.2	11.1
	MRCI	6.7	—	0	—	11.5
K	HF	21.6	22.7	0	—	4.1(#)
	CCSD(T)	18.3	19.3	0	—	13.0(#)
Rb	HF	21.6	22.2	0	—	22.2(#)
	CCSD(T)	18.3	18.8	0	—	12.5(#)
Cs	HF	22.0	22.1	0	—	3.9(#)
	CCSD(T)	18.6	18.8	0	—	11.3(#)
Fr	HF	21.4	21.5	0	—	4.1(#)
	CCSD(T)	18.5	18.5	0	—	11.9(#)
Cu	HF	0	—	39.4(#)	—	7.8
	CCSD(T)	0	—	57.0(#)	—	38.7
Ag	HF	0	—	31.2(#)	—	27.8
	CCSD(T)	0	—	63.9(#)	—	59.9
Au	HF	0	—	88.7(#)	—	69.6
	CCSD(T)	0	—	131.0(#)	—	109.2

^aFrom Ref. 5.

stability and the barrier height also increase as the level of the correlation effect included in the calculation becomes higher in the order HF → CCSD → CCSD(T).

The equilibrium internuclear distances are reported in Table II. It appears that the C–N distances in the metal complexes vary little from one complex to another and are found between 117 and 118 pm, about the bond length of free CN (117.2 pm) or CN[−] (117.7 pm). This is in agreement with Leroi and Klemperer’s ω_3 observations.⁷ In the triangular conformer of the alkali cyanide, the M–N distance is smaller than the M–C distance. The scalar relativistic effect in HF approximation shortens the M–N distance insignificantly (by a maximum of 2 pm in FrCN) and shortens the M–C distance slightly (by a maximum of 10 pm in FrCN). It is interesting to note that the correlation effect enlarges systematically the M–N and C–N distances while it shortens the M–C distance for the triangular (η^2) conformers, and it enlarges the C–N distance and shortens the M–C distance for the linear MCN conformers. It is as if the electron correlation made the steric repulsion from the C (2s²) electron pair weaker. The correlation effect makes the C–N distances larger and the M–C distances smaller for the linear MCN noble metal complexes as in the alkali complexes. The rotational frequencies are reported in Table III. Our calculated values are in good agreement with the experimentally measured values.

The harmonic vibrational frequencies of MCN com-

plexes are reported in Table IV. Concerning the discrepancy between Leroi and Klemperer’s ν_1 values⁷ and those of Ismail *et al.*,⁹ our result is closer to the latter. The decreasing tendency of the bending frequency (ω_1) for the Li → Na → K → Rb → Cs → Fr suite is in parallel with the decreasing bond energy or decreasing curvature of the potential energy surface near the equilibrium geometry for the same suite. For the doubly degenerate bending frequency (ω_2), the low stretching frequency (ω_1) and the high stretching frequency (ω_3) of the linear MCN of the Cu → Ag → Au suite, the AgCN has the smallest values and the CuCN has the largest values. A DFT calculation by Dietz *et al.*²⁰ also gave the same order for the vibrational frequencies. The ω_1 for AgCN was observed to be smaller than that of CuCN in the photoelectron detachment spectra of anions.¹⁹ This order indirectly suggests smaller M–CN bond energy for the AgCN than those of CuCN and AuCN.

The MCN complexes have large dipole moments created by the electron transfer from the metal atom to the CN group. The dipole moment of the NaCN is shown in Fig. 2. In this figure, r is fixed to 2.21 bohrs, R is fixed to 4.50 bohrs and only θ is varied. In this figure, the origin of the coordinates is placed at the center of mass of CN, the arrowheads point to the direction of the Li nucleus (indicated by “x”), and the lengths of vector are proportional to the amplitudes of dipole moment. Then we find that the dipole

TABLE II. Equilibrium bond lengths of the triangular η^2 (M[CN]) and the linear η^1 MCN complexes (in pm).

Metal	Conformer	Method	$R(\text{M}-\text{C})$	$R(\text{M}-\text{N})$	$R(\text{C}-\text{N})$
Li	η^2	CCSD(T)	213	185	118
		MRCI-2	209	186	117
		Expt. ^a		176.0	116.8
Na		CCSD(T)	239	223	118
		MRCI	272	226	117
		Expt. ^b	238	223	117
K		CCSD(T)	273	255	118
		MRCI	286	259	117
		Expt. ^c	272	255	117
Rb		CCSD(T)	286	268	118
Cs		CCSD(T)	303	282	118
Fr		CCSD(T)	309	289	118
Li	η^1	CCSD(T)	192		117
		MRCI	192		117
Na		CCSD(T)	225		117
		MRCI	291		117
K		CCSD(T)	260		117
Rb		CCSD(T)	273		117
Cs		CCSD(T)	288		117
Fr		CCSD(T)	294		117
Cu		CCSD(T)	184		117
		BP86/TZP ^d	178		117
		CCSD(T) ^e	186		118
		Expt. ^f	183		116
Ag		CCSD(T)	203		117
		BP86/TZP ^d	201		117
Au		CCSD(T)	192		117
		BP86/TZP ^d	192		117

^aFrom Ref. 10, supposedly LiNC linear.^bFrom Ref. 10.^cFrom Ref. 10, triangular structure.^dFrom Ref. 20.^eFrom Ref. 19.^fFrom Ref. 22.

moment vectors cut the line segment between the C and N atoms. This proves that the dipole moments can be simulated very well by two point charges (a point-charge dipole), one placed at the Na nucleus and the other one placed on the line connecting C and N atoms which is close to the center of mass of CN.

The molecular dipole moment can also be simulated by a three-point-charge system each placed at the center of atom (nucleus) according to the analysis explained in Sec. II. In the triangular LiCN case, for example, Li has an effective charge of +0.766, C has -0.440, and N has -0.327 in the MRCI, as can be seen in Table V where the effective charges for the triangular complexes of [(Li)-(Cs)]CN are calculated. For the linear molecules, [(Cu)-(Au)]CN, we cannot obtain the effective charges for all three atoms but two ef-

fective charges (e.g., those of C and N in this table) can be expressed in terms of the unknown third atomic charge (given by the positive metal atomic charges α , β , and γ in this table). Larger negative charge of the C atom in comparison with the N atom is in agreement with Fig. 2, where we see the negative charge shifts towards the C atom from the midpoint of C-N. This may contradict the commonly accepted notion that the N atom is more electronegative than the C atom, but the effective charge of C is more negative than N in CN⁻ anion due to the larger electron affinity of C than that of N. We can compare this with the MCO cases.³² The small dipole moment of the CO shows the carbon atom negative although the electron affinity of oxygen atom is larger than that of the carbon atom. In making a complex with a metal atom, the metal electron has a larger probability

TABLE III. Rotational constants of the MCN (in MHz).

Metal	Conformer	Method	<i>A</i>	<i>B</i>	<i>C</i>
⁷ Li	Linear LiNC	Present		13 061	
		Expt. ^a		13 293	
⁶³ Cu	Linear MCN	Present		4192	
		Expt. ^b		4225	
¹⁰⁷ Ag	Triangular (<i>η</i> ²)	Present		3233	
¹⁹⁷ Au		Present		3205	
²³ Na		Present	569 48	8310	7252
		Expt. ^c	579 22	8369	7273
³⁹ K		Present	572 45	4907	4519
		Expt. ^d	582 66	4940	4536
⁸⁵ Rb		Present	573 61	3481	3281
¹³³ Cs		Present	578 67	2838	2706
²²³ Fr		Present	575 55	2538	2431

^aFrom Ref. 10.^bFrom Ref. 22.^cFrom Ref. 10.^dFrom Ref. 11.

to stay around the carbon atom than around the oxygen atom. One may note that the MRCI gives a larger dipole moment than the CCSD(T) method. Although the dipole moment increases for the suite Li→Fr, it is about constant for Rb→Fr. Consequently, the effective charge of the metal atom (positive) shows a curious tendency. It increases for the suite Li→K then decreases for K→Fr, contrary to the commonly accepted electropositivity order. The effective charges of the nitrogen and carbon atoms, both negative, show the opposite tendency. The similar tendency is observed for the Mulliken charges derived from the natural MOs. Besides, the special relativistic effects significantly reduce ionization potentials for heavy elements. The internuclear distances, which will be less affected by the relativistic effect for these molecules, are probably the major factor for this deviation from the simple trend because the all-electron nonrelativistic HF calculation gave the same tendency. For the linear MCN complexes, the effective charge of the carbon atom should be more negative than that of the nitrogen atom if the effective charge of the metal atom is larger than a given positive number, that is, $Q_M > 2\mu(2r_{MC} + r_{CN})^{-1}$, where Q_M is the effective charge of the metal atom, μ is the dipole moment, r_{MC} is the distance between the metal atom and the carbon atom, and r_{CN} is the distance between the carbon atom and the nitrogen atom. This critical charge is 0.631 for Cu, 0.618 for Ag, and 0.509 for Au in atomic unit. The effective charges of the triangular forms calculated around the linear form suggest that this condition is satisfied for Cu and Ag but not for Au. If on the contrary the metal charge is smaller than the critical value, then the nitrogen atom should have more negative charge than that of the carbon atom. For the [(Cu)–(Au)]CN linear complexes the AuCN has the smallest dipole moment and AgCN has the largest one. This is believed to be connected with the large relativistic effect of the AuCN complex.

The potential contour map for NaCN is reported in Fig. 1(c), where $r(\text{C–N})$ is fixed to 2.21 bohrs and R and θ were varied. Here, θ should vary between 0° and 180° . The data outside this domain were added for a technical reason: that the equipotential lines should cut the $\theta=0^\circ$ and $\theta=180^\circ$ lines orthogonally. At very low collision energies, as the distance (R) between the Na atom and the center of mass of CN decreases from ∞ , the CN group should approach the sodium atom with the nitrogen atom heading to the sodium atom to follow the lowest energy path ($\theta \approx 180^\circ$). At small R , the CN moiety rotates around the sodium atom to make the triangular conformer. Along the path with the carbon atom heading to the sodium atom ($\theta \approx 0^\circ$), there exists a potential barrier. The same is valid for other MCN complexes of alkali atoms.

IV. CONCLUSION

In this paper, we have studied the molecular properties of the MCN complexes and surveyed the potential energy surfaces for the collision between the CN group and a metal atom M (groups 1 and 11). We find that the triangular conformer generally has the lowest energy in comparison with the linear cyanide and linear isocyanide for the complexes of alkali atoms. In the triangular complexes, the M–N distance is significantly shorter than the M–C distance. The potential barrier connecting the triangular form and the linear cyanide form decreases according to the order Li→Fr. The electron correlation effect enlarges the M–N and C–N distances and shortens the M–C distance for the alkali complexes, which can be attributed to a diminishment of the steric repulsion of the polarized nonbonding electron pair of the carbon atom. The MCN complexes have large dipole moments. The effective charge of the metal atom shows a curious tendency, in-

TABLE IV. Harmonic vibrational frequencies (in cm^{-1}) of MCN calculated by CCSD(T) method compared with other data.

Metal	Conformer	Method	ω_2	ω_1	ω_3
^7Li	Linear LiNC	CCSD(T)	113	706	2082
		Expt. ^a	120	681	2080
	Triangular η^2	CCSD(T)	181	656	2040
	Linear LiCN	CCSD(T)	180	623	2142
^{23}Na	Triangular η^2	CCSD(T)	187	379	2043
		Expt. ^b	239		2176
		Expt. ^a	168	368	2047
		Expt. ^c	179		
^{39}K		CCSD(T)	166	299	2048
		Expt. ^b	207		2158
		Expt. ^a	139	288	2050
		Expt. ^c	157		
^{85}Rb		CCSD(T)	153	255	2048
^{133}Cs		CCSD(T)	134	234	2047
^{223}Fr		CCSD(T)	136	224	2045
^{63}Cu	Linear MCN	CCSD(T)	336	519	2190
		BP86/TZP ^d	255	512	2177
		CCSD(T) ^e	225	453	2159
		Expt. ^f	270	478	
^{107}Ag		CCSD(T)	186	395	2168
		BP86/TZP ^d	224	397	2171
		Expt. ^e		390	
^{197}Au		CCSD(T)	259	478	2179
		BP86/TZP ^d	292	475	2176

^aFrom Ref. 9.^bFrom Ref. 7.^cFrom Ref. 10.^dFrom Ref. 20.^eFrom Ref. 19.^fFrom Ref. 22.

creasing for the suite $\text{Li} \rightarrow \text{K}$ then decreasing for $\text{K} \rightarrow \text{Fr}$. The carbon atom has a larger negative charge than that of the nitrogen atom in the alkali complexes. For a very low energy collision between the alkali atom and the CN group, it is energetically most probable that the nitrogen atom of the CN group makes a head-on collision with the metal atom, then the CN group rotates at short distances to assume a triangular

form. The noble metal atoms prefer the linear cyanide form to the linear isocyanide form. The barrier connecting those two conformers increases according to the order $\text{Cu} < \text{Ag} < \text{Au}$. The vibrational frequencies show minima for the AgCN in comparison with CuCN and AuCN , suggesting probably the smallest bond energy for AgCN among those complexes. The $r_e(\text{C}-\text{N})$ varies little for different species

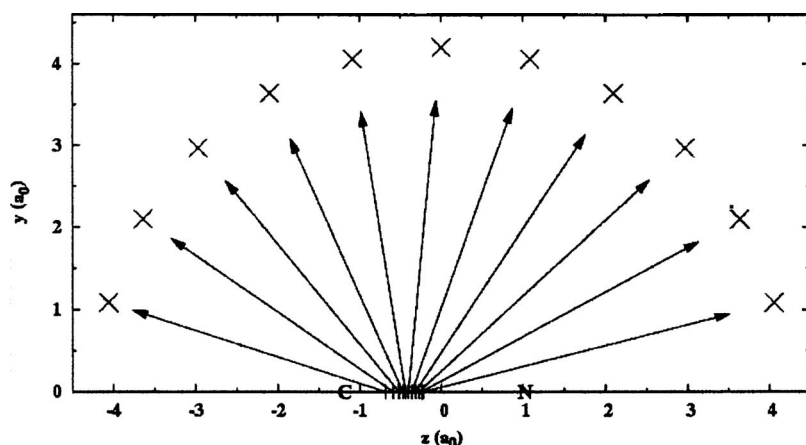


FIG. 2. Dipole moment vectors of LiCN as a function of θ with $r(\text{C}-\text{N})=2.21$ bohrs and $R=4.50$ bohrs. The CN group lies along the abscissa, the $\text{C} \rightarrow \text{N}$ direction is taken positive, with its center of mass coinciding with the origin of coordinates. The arrowheads of the dipole moment vectors point to the direction of the Li nucleus (indicated by "x"), and the lengths of vector are proportional to the amplitudes of dipole moment.

TABLE V. Dipole moments and effective atomic charges of the MCN, triangular (η^3) complexes for [(Li)–(Cs)]CN, and linear complexes for [(Cu)–(Ag)]CN, calculated from the dipole moment (in atomic units, 1 a.u. of dipole moment is equivalent to 2.541 75 D). The effective charges α , β , and γ should be real numbers between 0 and 1.

Metal	Method	DM	$Q(M)$	$Q(N)$	$Q(C)$
Li	CCSD(T)	2.6775	0.765	–0.363	–0.402
	MRCI-2	2.7644	0.766	–0.327	–0.440
Na	CCSD(T)	3.4757	0.820	–0.372	–0.448
	MRCI	3.6313	0.843	–0.321	–0.522
K	CCSD(T)	4.0444	0.828	–0.368	–0.460
	MRCI ^a	4.4963	0.884	–0.317	–0.567
Rb	CCSD(T)	4.1697	0.812	–0.358	–0.454
Cs	CCSD(T)	4.2667	0.784	–0.342	–0.442
Fr	CCSD(T)	4.2761	0.768	–0.333	–0.435
Cu	CCSD(T)	2.8911	α	$1.573\alpha - 1.308$	$1.308 - 2.573\alpha$
Ag	CCSD(T)	3.0535	β	$1.735\beta - 1.381$	$1.381 - 2.735\beta$
Au	CCSD(T)	2.4075	γ	$1.641\gamma - 1.089$	$1.089 - 2.641\gamma$

^aAll-electron nonrelativistic data.

and remains around the bond distances of free CN and CN[–]. The relativistic effects of the MCN complexes are under more comprehensive investigation.

ACKNOWLEDGMENTS

This work was supported by the Korea Research Foundation Grant funded by the Korean Government (MOEHRD) (KRF-2006-312-C00191) in which computational resources were provided by the Supercomputing Center of the Korea Institute of Science Technology Information (KISTI), a grant (06K1401-01010) from Center for Nanoscale Mechatronics and Manufacturing, one of the 21st Century Frontier Research Programs which are supported by Ministry of Science and Technology, Korea, and the CNRS through the IDRIS, Orsay (Project 051825). One of the authors (G.H.J.) would like to thank the KOFST for the support through the Brain Pool Program 2005. Another author (D.H.R.) would like to thank the Chemistry Department of the KAIST for hospital-ity during his stay in 2005.

¹M. L. Klein, J. D. Goddard, and D. G. Bounds, J. Chem. Phys. **75**, 3909 (1981).

²P. E. S. Wormer and J. Tennyson, J. Chem. Phys. **75**, 1245 (1981). R. Esser, J. Tennyson, and P. E. S. Wormer, Chem. Phys. Lett. **89**, 223 (1982).

³C. J. Marsden, J. Chem. Phys. **76**, 6451 (1982).

⁴P. R. von Schleyer, A. Sawaryn, E. A. Reed, and P. Hobza, J. Comput. Chem. **7**, 666 (1986).

⁵J. Makarewicz and T.-K. Ha, Chem. Phys. Lett. **232**, 497 (1995).

⁶S. Petrie, J. Phys. Chem. **100**, 11581 (1996); Phys. Chem. Chem. Phys. **1**, 2897 (1999).

⁷G. E. Leroi and W. Klemperer, J. Chem. Phys. **35**, 774 (1961).

⁸Chemistry Webbook from the NIST website (<http://nist.gov/>).

⁹Z. K. Ismail, R. H. Hauge, and J. L. Margrave, J. Chem. Phys. **57**, 5137 (1972); J. Mol. Spectrosc. **45**, 304 (1973); J. Mol. Spectrosc. **54**, 402 (1975).

¹⁰J. J. van Vaals, W. Leo Meerts, and A. Dymanus, Chem. Phys. **82**, 385 (1983); Chem. Phys. **86**, 147 (1984).

¹¹T. Törring, J. P. Bekooy, W. Leo Meerts, J. Hoeft, E. Tiemann, and A. Dymanus, J. Chem. Phys. **73**, 4875 (1980).

¹²L. T. Redmon, G. D. Purvis III, and R. J. Bartlett, J. Chem. Phys. **72**, 986 (1980).

¹³V. S. Rao, A. Vijay, and A. K. Chandra, Can. J. Chem. **74**, 1072 (1996).

¹⁴S. C. Farantos and J. Tennyson, J. Chem. Phys. **82**, 800 (1985).

¹⁵C. J. Nelin, P. S. Bagus, and M. R. Philpott, J. Chem. Phys. **87**, 2170 (1987).

¹⁶I. Garcia Cuesta, A. Sanchez de Meras, and I. Nebot-Gil, Chem. Phys. **170**, 1 (1993).

¹⁷A. Veldkamp and G. Frenking, Organometallics **12**, 4613 (1993).

¹⁸L. Bouslama, A. Daoudi, H. Mestdagh, C. Rolando, and M. Suard, J. Mol. Struct.: THEOCHEM **330**, 187 (1995).

¹⁹A. I. Boldyrev, X. Li, and L.-S. Wang, J. Chem. Phys. **112**, 3627 (2000).

²⁰O. Dietz, V. M. Rayon, and G. Frenking, Inorg. Chem. **42**, 4977 (2003).

²¹C. W. Bauschlicher, Jr., Surf. Sci. **154**, 70 (1985).

²²D. B. Grotjahn, M. A. Brewster, and L. M. Ziurys, J. Am. Chem. Soc. **124**, 5895 (2002).

²³A. Paul, Y. Yamaguchi, H. F. Schaefer III, and K. A. Peterson, J. Chem. Phys. **124**, 034310 (2006).

²⁴B. Bak, E. Clementi, and R. N. Kortzeborn, J. Chem. Phys. **52**, 764 (1970); E. Clementi, H. Kistenmacher, and H. Popkie, *ibid.* **58**, 2460 (1973).

²⁵D.-K. Lee, Y. S. Lee, D. Hagebaum-Reignier, and G.-H. Jeung, Chem. Phys. **327**, 406 (2006); G.-H. Jeung, Theor. Chem. Acc. **116**, 450 (2006).

²⁶K. Andersson, F. Aquilante, M. Barysz *et al.*, MOLCAS, University of Lund, 1997.

²⁷H.-J. Werner, P. J. Knowles, R. Lindh *et al.*, MOLCAS, Stuttgart University and Cardiff University, 2000.

²⁸M. J. Frisch G. W. Trucks, H. B. Schlegel *et al.*, GAUSSIAN, Gaussian, Inc., Pittsburgh, PA, 2003.

²⁹I. S. Lim, P. Schwerdtfeger, B. Metz, and H. Stoll, J. Chem. Phys. **122**, 104103 (2005).

³⁰D. Figgen, G. Rauhut, M. Dolg, and H. Stoll, Chem. Phys. **311**, 227 (2005).

³¹S. E. Bradforth, E. H. Kim, and D. W. Arnold, J. Chem. Phys. **98**, 800 (1993).

³²G.-H. Jeung, J. Am. Chem. Soc. **114**, 3211 (1992); G. H. Jeung and J. Koutecký, Chem. Phys. Lett. **129**, 569 (1986).